Inorganic Chemistry

COMMUNICATION

pubs.acs.org/IC

Magnetic Properties of a Manganese(III) Chain with Monoatomic Bridges: *catena*-MnF(salen)

Torben Birk, Kasper S. Pedersen, Stergios Piligkos, Christian Aa. Thuesen, Högni Weihe, and Jesper Bendix*

Department of Chemistry, University of Copenhagen, Universitetsparken 5, DK-2100 Copenhagen, Denmark

Supporting Information

ABSTRACT: In the solid state, MnF(salen) forms chains wherein fairly linear fluoride bridges between high-spin Mn^{III} centers are observed. We interpret the magnetic properties of these chains by use of the classical Fisher model and by use of the high-temperature expansion approach, as well as by exact matrix diagonalization of the spin Hamiltonian, of model rings. In solution, electron paramagnetic resonance shows the chains to be symmetrically cleaved to monomeric MnF(salen).

In recent years, the fluoride ligand has received increasing focus as a bridging ligand for incorporation in magnetic materials because of its spectroscopic and redox innocence and because it exhibits a distinct preference to forming linear bridges, providing thus the means for cluster design.[1] Surprisingly, the most ubiquitous building block[2] in molecule-based magnetic systems such as single-molecule[3,4b] and single-chain magnets,[4] Mn^{III}(salen)$^+$ has not been structurally or magnetically investigated with fluoride coligands. The synthesis of the title compound from MnF_3 and H_2salen, in methanol, is straightforward (Supporting Information, SI). The chain structure of **1** is shown in Figure 1. In **1**, the equatorial Schiff-base coordination resembles that found in other Mn^{III}(salen) complexes.[2,5] The propensity of fluoride for forming linear bridges and the steric demands of the salen ligand result in the linear chain structure of **1** in which three crystallographically inequivalent Mn^{III} atoms exist in the unit cell ($P\bar{1}$) and three different bridging Mn−F−Mn angles are observed, namely, 150.43(4)° (Mn2−F3−Mn3), 151.72(3)° (Mn1−F2−Mn2), and 180.0° (Mn1−F1−Mn1 and Mn3−F4−Mn3). In the crystal structure of **1**, the F atoms labeled F1 and F4 are located on inversion centers. Similar linear fluoride bridges are observed in [V(O)(salen)(μ-F)V(O)(salen)](BF_4), wherein V−F−V angles range from 171.96° to 173.50°.[6] A comparison of the Mn−F bond lengths in **1** with the bond lengths in MnF_3 shows that the Mn^{III} centers in **1** are tetragonally elongated by Jahn−Teller distortion.[7]

The formation of chains from the association of Mn^{III}(salen)$^+$ fragments with polyatomic bridges has been frequently observed, e.g., in Mn(X)(salen) (where X = CH_3COO, NO_3, CN, N_3).[8] However, only a few examples of dimers of Mn^{III}(salen) units linked by monatomic bridges have been characterized, and chains of M(salen) complexes with monatomic bridges have not been reported for any metal centers.[9]

The magnetic moment of **1** was measured in the temperature range 1.8−370 K in a 1 kOe direct-current magnetic field. The obtained data are shown in Figure 2 in the form of magnetic susceptibility, χ, and of the χT product. In Figure 2 are also shown the results obtained from modeling of the magnetic data by use of various approaches. The high-temperature value of the χT product (1.84 cm^3 K mol^{-1} at 370 K) is significantly lower than the value expected for an isolated high-spin Mn^{III} ion (3.00 cm^3 K mol^{-1} for g = 2). Upon cooling, the χT product steadily decreases to a minimum value of 0.01 cm^3 K mol^{-1} at 1.8 K. These two observations imply dominant antiferromagnetic intrachain interactions between the manganese centers. This conclusion is further supported by the observation that magnetization of **1** at T = 1.8 K does not saturate at a field of 50 kOe (see the SI, Figure SI1), as was expected for strongly antiferromagnetically coupled systems.

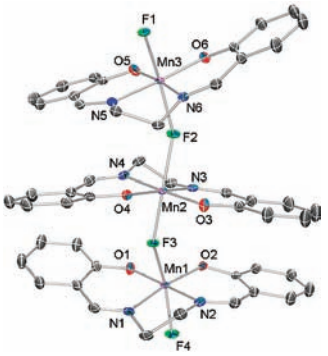

Figure 1. Molecular structure of MnF(salen). Displacement ellipsoids are drawn at 50% probability. H atoms are omitted for clarity. Bond length intervals (Å): Mn−O 1.8925(8)−1.9119(9), Mn−N 1.9949(9)−2.0059(8), Mn−F 2.049(2)−2.096(2). Angle intervals (deg): Mn−F−Mn 150.43(4)−180.0.

The χT product of **1** shows no evidence of spin-canting behavior, which would be manifested by a slight increase of χT at low temperatures.[10] In fact, the existence of the inversion center in the chain structure of **1**, in conjuction with the topology of the three inequivalent Mn^{III} centers in the asymmetric unit of **1**, results in the complete cancellation of local magnetic moments. This is further explained by qualitative arguments in Figure SI2 of the SI. However, a residual magnetization persists at low temperatures, as can be seen in Figures 2 and SI1 of the SI. This residual magnetization can be due to small amounts of monomeric Mn^{III} impurities. Finally, alternating-current susceptibility measurements down to 1.8 K do not reveal slow relaxation of the magnetization behavior or the presence of a magnetic phase transition.

Received: February 8, 2011
Published: May 19, 2011

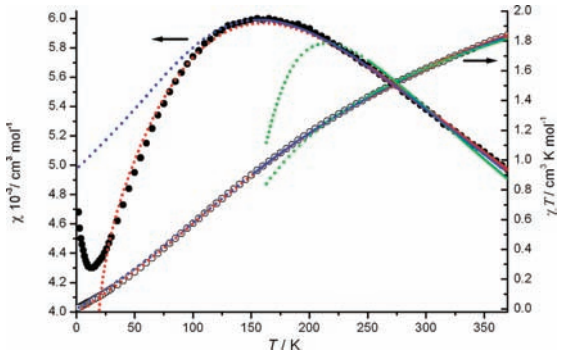

Figure 2. Magnetic susceptibility and χT product data for **1**. Solid and hollow circles correspond to experimental susceptibility and χT product data, respectively. The theoretical best-fit curves obtained in the temperature range 370−250 K by full-matrix diagonalization of nonanuclear models and by high-temperature expansion and in the temperature range 370−100 K by the Fisher model are shown as solid red, green, and blue lines, respectively. Extensions of these curves at lower temperatures, using the best-fit J parameter, are shown as dotted lines.

We used various models for interpretation of the magnetization data of **1**, namely, the classical Fisher model[11] and the quantum-mechanical models of high-temperature expansion[12] and of the exact matrix diagonalization of the spin Hamiltonian, of model systems. Within the Fisher model, the analytical expression for the magnetic susceptibility of an infinite chain of classical spins is derived. The magnetic susceptibility of **1** was fitted to the isotropic spin Hamiltonian (1)

$$\hat{H} = J\sum_{1}^{N}\hat{S}_i\cdot\hat{S}_{i+1} + \sum_{1}^{N}\mu_B B g\hat{S}_i \qquad (1)$$

by use of the analytical expression (2), giving the magnetic susceptibility of an infinite chain of classical spins, derived by Fisher.

$$\chi = \frac{N_A g^2\mu_B S(S+1)}{3k_B T}\frac{1+u}{1-u};$$
$$u = \coth\left(-\frac{6J}{k_B T}\right) + \frac{k_B T}{6J} \qquad (2)$$

A satisfactory fit to the experimental data was obtained only down to temperatures of about 100 K (Figure 2). At temperatures lower than 100 K, the classical Fisher model fails because at low temperatures quantum effects gain importance. The exchange-coupling interaction was found to be $J = 38$ cm^{-1} (for $g = 2$), comparable to purely inorganic one-dimensional fluoride-bridged Mn^{III} systems based on *trans*-$[MnF_4F_{2/2}]^{2-}$ units.[13] The only structurally characterized example of chloride-bridged Mn^{III} chains is *catena*-Mn(bipy)Cl_3, which has longer (2.503−2.763 Å) and more bent (135.09°) bridges with concomitant weaker coupling: $J \approx 24$ cm^{-1}.[14]

Interpretation of the magnetic properties of **1** by exact quantum treatment is impossible, given that, except in the case of antiferromagnetic spin half-chains,[15] no analytical solution exists for this problem for infinite systems. Thus, we followed an approach based on extrapolation to infinity of the results obtained, by exact or high-temperature expansion treatments, on increasing dimension model systems. This general strategy was first presented in pioneering work by Bonner and Fisher.[11b] The model systems that we use herein are antiferromagnetically coupled rings consisting of Mn^{III} ions presenting only first-neighbor interactions, as expressed by (1).

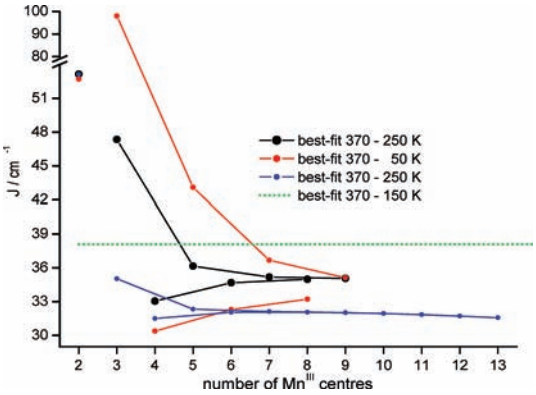

Figure 3. Isotropic exchange, J, values determined by fitting the experimental data to various ring sizes and models (black and red, full-matrix diagonalization; blue, high-temperature expansion; green, Fisher model).

The high-temperature expansion approach consists of computation of the partition function of the system by use of a series expansion of the exponential of the thermally weighted spin Hamiltonian of the system. A brief description of this approach is given in the SI. The details of our implementation of this approach have been discussed elsewhere.[16] By use of the high-temperature expansion up to the 13th order, for our model ring systems, we were able to fit the experimental data in the temperature range 370−250 K (Figure 2). At lower temperatures, the 13th-order high-temperature expansion is not sufficient to accurately describe the magnetic properties of **1**. Higher order expansions are needed for this purpose. However, this is computationally very demanding. The best-fit J parameters (for $g = 2$) determined by the high-temperature expansion approach for model systems of nuclearity ranging from 2 to 13 are shown in Figure 3. The theoretical curves obtained from the best-fit J parameter in the case of a nonanuclear ring are shown as solid lines in Figure 2, where is also shown the extension of these theoretical curves at lower temperatures (dotted lines). The best-fit J parameters determined by the high-temperature expansion approach asymptotically converge to a limit of about 32 cm^{-1}, as the nuclearity increases. This limit corresponds to the antiferromagnetic exchange interaction in the infinite chain. However, with increasing nuclearity, a slight divergence from this limit is observed (Figure 3). This reflects the fact that, at constant expansion order (here the 13th order), the model becomes less accurate as the nuclearity increases. This is further illustrated by the fact that only for a dinuclear system the result obtained by the high-temperature expansion exactly matches the solution obtained by full-matrix diagonalization.

The best-fit J parameters (for $g = 2$) determined, in two different temperature ranges, by full-matrix diagonalization of the spin Hamiltonian (1) for model systems of nuclearity ranging from 2 to 9 are also shown in Figure 3. Our analysis was limited to nuclearity 9 because we block-diagonalized the isotropic exchange spin Hamiltonian (1) by exploiting only the symmetries related to the total spin, S, and its projections along the quantization axis, S_z. As in the case of the high-temperature expansion, the determined values of J converge asymptotically toward a limit with increasing nuclearity. In the case that the fit has been performed in the same temperature range as that for the high-temperature

dx.doi.org/10.1021/ic2002699 |*Inorg. Chem.* 2011, 50, 5312–5314

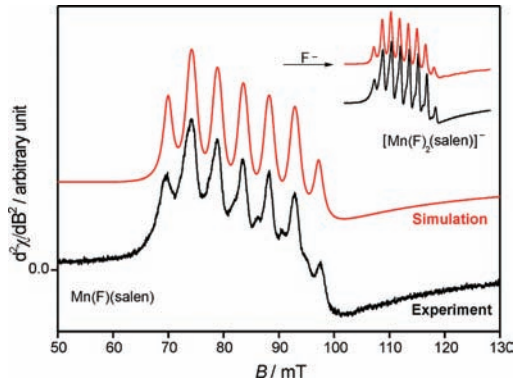

Figure 4. Parallel-mode EPR spectrum of Mn(F)(salen) in frozen NMF glass at T = 5.65 K and ν = 9.416 425 GHz. The inset shows the effect of the addition of excess F^-. Simulation parameters (for Hamiltonian, see ref 16): [Mn(F)(salen)], g_z = 7.92 cm^{-1}, Δ = 0.0555 cm^{-1}, A_z = 0.017 25 cm^{-1}, $A_{z,ax}$ = 0.0145 cm^{-1}; *trans*-[MnF_2(salen)]$^-$, g_z = 7.92 cm^{-1}, Δ = 0.071 30 cm^{-1}, A_z = 0.017 60 cm^{-1}, $A_{z,ax}$ = 0.016 95 cm^{-1}.

expansion (370−250 K), the antiferromagnetic exchange interaction is estimated at around 35 cm^{-1}. In the case that the fit is extended at lower temperatures (370−50 K), the determined antiferromagnetic exchange interaction is estimated at around 34 cm^{-1}. For the sake of clarity, only the curves related to the full-matrix diagonalization fit in the temperature range 370−250 K are shown in Figure 3, in the case of a nonanuclear ring. However, the corresponding curves obtained by full-matrix diagonalization fit in the temperature range 370−50 K are very similar to the ones shown in Figure 2 because the J values determined for the nonanuclear rings in the two temperature ranges are very similar (Figure 3).

We recently found that parallel-mode electron paramagnetic resonance (EPR) on frozen glasses is capable of resolving superhyperfine couplings to fluoride bound to Mn^{III} in MnF_6^{3-}.[17] These Jahn−Teller-distorted systems are characterized by strongly anisotropic superhyperfine couplings, with the coupling to the distant fluorides on the Jahn−Teller-elongated axis being much larger (by a factor of ca. 4) than the coupling to the more closely bound equatorial fluorides. Application of this knowledge to the parallel-mode EPR of NMF solutions of **1** clearly demonstrates that the chain upon dissolution forms neutral [MnF(salen)] with undetectable amounts of complexes with more than one fluoride ligand (cf. Figure 4). The addition of excess F^- to the NMF solution before freezing yields clean conversion to *trans*-[MnF_2(salen)]$^-$.

■ ASSOCIATED CONTENT

Supporting Information. X-ray structure data (CCDC 796782), outline of the methodology used in the high-temperature expansions, additional magnetic data, and experimental procedures. This material is available free of charge via the Internet at http://pubs.acs.org.

■ AUTHOR INFORMATION

Corresponding Author
*E-mail: bendix@kiku.dk.

■ ACKNOWLEDGMENT

K.S.P. thanks DANSCATT for financial support. S.P. thanks the Danish Natural Science Research Council for a Steno grant.

■ REFERENCES

(1) (a) Larsen, F. K.; McInnes, E. J. L.; Mkami, H. E.; Overgaard, J.; Piligkos, S.; Rajaraman, G.; Rentschler, E.; Smith, A. A.; Smith, G. M.; Boote, V.; Jennings, M.; Timco, G. A.; Winpenny, R. E. P. *Angew. Chem., Int. Ed.* **2003**, *42*, 101–105. (b) Affronte, M.; Carretta, S.; Timco, G. A.; Winpenny, R. E. P. *Chem. Commun.* **2007**, 1789–1797. (c) Meally, S. T.; Mason, K.; McArdle, P.; Brechin, E. K.; Ryder, A. G.; Jones, L. F. *Chem. Commun.* **2009**, 7024–7026. (d) Birk, T.; Schau-Magnussen, M.; Piligkos, S.; Weihe, H.; Holten, A.; Bendix, J. *J. Fluorine Chem.* **2010**, *131*, 898–906.

(2) Miyasaka, H.; Saitoh, A.; Abe, S. *Coord. Chem. Rev.* **2007**, *251*, 2622–2664.

(3) (a) Gatteschi, D.; Sessoli, R. *Angew. Chem.* **2003**, *115*, 278–309. (b) Miyasaka, H.; Clérac, R.; Wernsdorfer, W.; Lecren, L.; Bonhomme, C.; Sugiura, K.-I.; Yamashita, M. *Angew. Chem.* **2004**, *116*, 2861–2865. (c) Pedersen, K. S.; Schau-Magnussen, M.; Bendix, J.; Weihe, H.; Palii, A. V.; Klokishner, S. I.; Ostrovsky, S.; Reu, O. S.; Mutka, H.; Tregenna-Piggott, P. L. W. *Chem.—Eur. J.* **2010**, *16*, 13458–13464.

(4) (a) Clérac, R.; Miyasaka, H.; Yamashita, M.; Coulon, C. *J. Am. Chem. Soc.* **2002**, *124*, 12837–12844. (b) Ferbinteanu, M.; Miyasaka, H.; Wernsdorfer, W.; Nakata, K.; Sugiura, K.; Yamashita, M.; Coulon, C.; Clérac, R. *J. Am. Chem. Soc.* **2005**, *127*, 3090–3099.

(5) (a) Darensbourg, D. J.; Frantz, E. B. *Dalton Trans.* **2008**, 5031–5036. (b) Ni, Z.-H.; Kou, H.-Z.; Zhang, L.-F.; Ge, C.; Cui, A.-L.; Wang, R.-J.; Li, Y.; Sato, O. *Angew. Chem., Int. Ed.* **2005**, *44*, 7742–7745.

(6) Fairhurst, S. A.; Hughes, D. L.; Leigh, G. J.; Sanders, J. R.; Weisner, J. *Dalton Trans.* **1994**, 2591–2598.

(7) Wells, A. F. *Structural Inorganic Chemistry*, 5th ed.; Clarendon Press: Oxford, U.K., 1984; p 324.

(8) (a) Davies, J. E.; Gatehouse, B. M.; Murray, K. S. *J. Chem. Soc., Dalton Trans.* **1973**, 2523–2527. (b) Shyu, H.-L.; Wei, H.-H.; Wang, Y. *Inorg. Chim. Acta* **1999**, *290*, 8–13. (c) Matsumoto, N.; Sunatsuki, Y.; Miyasaka, H.; Hashimoto, Y.; Luneau, D.; Tuchagues, J.-P. *Angew. Chem., Int. Ed.* **1999**, *38*, 171–173. (d) Ko, H. H.; Lim, J. H.; Kim, H. C.; Hong, C. S. *Inorg. Chem.* **2006**, *45*, 8847–8849. (e) Yuan, M.; Gao, S.; Sun, H.-L.; Su, G. *Inorg. Chem.* **2004**, *43*, 8221–8223.

(9) Liu, Y.; Dou, J.; Niu, M.; Zhang, X. *Acta Crystallogr., Sect. E* **2007**, *63*, m2771–m2771.

(10) Mossin, S.; Weihe, H.; Sorensen, H. O.; Lima, N.; Sessoli, R. *Dalton Trans.* **2004**, 632–639.

(11) (a) Fisher, M. E. *J. Am. Phys.* **1964**, *32*, 343–346. (b) Bonner, J. C.; Fisher, M. E. *Phys. Rev. A* **1964**, *135*, 640.

(12) (a) Rushbrooke, G. S.; Wood, P. J. *Mol. Phys.* **1958**, *1*, 257–283. (b) Eifert, T.; Hüning, F.; Lueken, H.; Schmidt, P.; Thiele, G. *Chem. Phys. Lett.* **2002**, *364*, 69–74. (c) Schmidt, H.-J.; Schnack, J.; Luban, M. *Phys. Rev. B* **2001**, *64*, 224415.

(13) Palacio, F.; Morón, M. C. In *Research Frontiers in Magnetochemistry*; O'Connor, C. J., Ed.; World Scientific: Singapore, 1993.

(14) (a) Perlepes, S. P.; Blackman, A. G.; Huffman, J. C.; Christou, G. C. *Inorg. Chem.* **1991**, *30*, 1665–1668. (b) Granroth, G. E.; Meisel, M. W.; Chaparala, M.; Jolicoeur, T.; Ward, B. H.; Talham, D. R. *Phys. Rev. Lett.* **1996**, *77*, 1616–1619.

(15) Bethe, H. A. *Z. Phys.* **1931**, *71*, 205–226.

(16) Thuesen, C. A.; Weihe, H.; Bendix, J.; Piligkos, S.; Mønsted, O. *Dalton Trans.* **2010**, *39*, 4882–4885.

(17) Scheifele, Q.; Birk, T.; Bendix, J.; Tregenna-Piggott, P. L. W.; Weihe, H. *Angew. Chem., Int. Ed.* **2008**, *47*, 148–150.